Mechanical and Microstructural Properties of Native Pediatric Posterior Cruciate and Collateral Ligaments

Elaine C. Schmidt,* MS, Matthew Chin,* BS, Julien T. Aoyama,† BA, Theodore J. Ganley,† MD, Kevin G. Shea,‡ MD, and Michael W. Hast,*§ PhD

Investigation performed at the Biedermann Laboratory for Orthopaedic Research, Department of Orthopaedic Surgery, University of Pennsylvania, Philadelphia, Pennsylvania, USA

Background: Although anterior cruciate ligament (ACL) tears have received the most attention, the medial collateral ligament (MCL) is thought to be the most commonly injured knee ligament overall. The lateral collateral ligament (LCL) and posterior collateral ligament (PCL) are less frequently compromised but can be involved in severe multiligament injuries. The paucity of information on the native properties of these ligaments in the pediatric population hinders the overall optimization of treatment for these injuries.

Purpose: To characterize the mechanical and microstructural properties of pediatric MCLs, LCLs, and PCLs using a rare cadaveric cohort (mean age, 9.2 years).

Study Design: Descriptive laboratory study.

Methods: MCLs, LCLs, and PCLs were harvested from 5 fresh-frozen pediatric knee specimens (3 male, 2 female) and were subjected to a tensile loading protocol. A subset of contralateral tissues from a single donor was analyzed using bright-field, polarized light, and transmission electron microscopy to measure collagen fiber morphology.

Results: The pediatric MCL exhibited values for ultimate stress (11.7 ± 6.7 MPa), ultimate strain (18.2% ± 6.8%), and the Young modulus (93.7 ± 56.5 MPa) that were similar to values for the LCL (11.4 ± 11.5 MPa, 27.7% ± 12.9%, and 64.4 ± 76.6 MPa, respectively). The PCL demonstrated decreased ultimate stress (4.2 ± 1.8 MPa), increased ultimate strain (28.8% ± 11.9%), and a decreased Young modulus (19.8 ± 10.4 MPa) when compared with the MCL and LCL. All 3 ligaments had similar mean crimp wavelengths (MCL, 32.8 ± 3.6 μm; LCL, 27.2 ± 3.5 μm; PCL, 25.8 ± 3.5 μm) and collagen fibril diameters (MCL, 88.0 ± 26.0 nm; LCL, 93.3 ± 34.6 nm; PCL, 90.9 ± 34.0 nm); however, the fibril distribution profiles exhibited different modalities.

Conclusion: The pediatric MCL and LCL possessed similar mechanical properties, while the pediatric PCL was weaker but capable of withstanding higher amounts of strain. All 3 of these pediatric structures were weaker than what has been reported in studies with adult cohorts.

Clinical Relevance: Results from this study can be considered preliminary mechanical and microstructural data for healthy pediatric collateral and posterior cruciate ligaments that can be used to guide further laboratory and clinical research.

Keywords: pediatric; MCL; LCL; PCL; mechanical properties; microstructural properties

Research into the mechanical and microstructural properties of human tendons and ligaments has been conducted almost exclusively with samples from adult donors. Relatively little is known about these properties in the pediatric population because of the limited availability of these cadaveric specimens. At the same time, there is a growing clinical need for comprehensive data regarding pediatric knee ligament repair and reconstruction. Because of the increase in youth sport participation and specialization, there has been a steady rise in the rates of diagnosed knee ligament tears in skeletally immature patients.[8,41] These injuries pose a serious burden on young athletes, their families, and the overall health care system, as treatment can require surgical repair and a lengthy recovery period.[20,24,41]

Medial collateral ligament (MCL) injuries occur either by direct lateral trauma (contact) or by pivoting maneuvers that create a large valgus moment across the knee joint (noncontact).[23] MCL tears have been shown to be one of the most prevalent sport-related knee injuries, with 1 epidemiological study reporting that they encompass 36.1% of all knee injuries among high school athletes.[41] Although some tears occur in combination with anterior cruciate ligament (ACL) tears, the majority of these injuries are isolated. The

The Orthopaedic Journal of Sports Medicine, 7(2), 2325967118824400
DOI: 10.1177/2325967118824400

MCL exhibits excellent healing capacity, and consequently, these injuries are often treated nonoperatively except in cases of severe multiligament injuries.

Injuries to the lateral collateral ligament (LCL) are less common and, as a result, are less often studied. LCL tears have been shown to possess inferior healing potential compared with the MCL, with grade 3 LCL tears usually necessitating surgery.[30] Surgical intervention is required when the LCL has been compromised in combination with a cruciate ligament. Postoperative varus instability, caused by a deficient LCL, has been shown to overload cruciate grafts to the point that graft failure may result.[27,28] Although little is known about the mechanical properties of the native tissue, LCL reconstruction using autologous semitendinosus grafts has been recommended and has shown good clinical outcomes.[29]

Posterior collateral ligament (PCL) injuries are also relatively rare and less well studied, particularly in the pediatric population.[3] Because of their asymptomatic nature, however, PCL tears may be more common than previously thought. PCL injuries can be caused by posteriorly directed force to the proximal tibia of the flexed knee, which most often occurs in sports and high-energy automobile accidents. In the pediatric population, PCL injuries rarely occur in the ligament intrasubstance; they more commonly present as osteochondral avulsions at either the tibial or femoral attachment.[15,16] Isolated partial PCL tears are commonly treated nonoperatively to minimize the risk of iatrogenic physeal injuries. Conversely, acute ligament injuries combined with bone avulsions or symptomatic high-grade tears require surgical intervention.[10] It has been shown that the PCL-deficient knee can alter knee kinematics, which consequently results in elevated joint contact pressure and degenerative changes to the patellofemoral and medial compartments of the knee.[3,11] Reconstructive techniques attempt to improve posterior laxity with either a single- or double-bundle PCL graft or a tibial inlay technique.[2] Several studies have shown that PCL reconstruction is a viable treatment option with good clinical outcomes in pediatric patients with multiligament injuries or those who are not responding to conservative treatment.[3,7,22]

Surgical repair of pediatric MCLs, LCLs, and PCLs can be improved by developing a more comprehensive understanding of the structural and biomechanical characteristics of the native tissues. In many ways, treatment of MCL, LCL, and PCL injuries in pediatric patients mimics the clinical modalities that are used in adults, but it is unclear if this paradigm is prudent. Graft choices for pediatric patients are similar to those for adult ACL repair and include hamstring, quadriceps, and patellar tendon grafts. Many in vitro studies have examined the material properties of MCLs, LCLs, and PCLs in adults[35,36,46] and skeletally immature animal models,[6,13,47] but to our knowledge, no analogous studies have been conducted for the pediatric population.

The goal of this study was to provide a detailed characterization of the mechanical properties and microstructure of pediatric knee ligaments. Knowledge of these properties for the pediatric MCL, LCL, and PCL may ultimately help to enhance the effectiveness of candidate graft selection to combat problems related to postoperative ligamentous balance of the knee.

METHODS

Fresh-frozen pediatric knee tissues from 5 cadaveric specimens (3 male, 2 female; mean age, 9.2 years) were obtained via donation from AlloSource and used in this study. There were no exclusion criteria for the donors, and all information related to activity level, medical history, and cause of death was blinded. Specimens were defrosted completely, and bone-ligament-bone segments were dissected away from the knee. For each donor, the MCL, LCL, and PCL from 1 knee were dissected, such that there were 15 ligament specimens in total for mechanical testing. The PCLs were dissected and mechanically tested as a single unit containing both anterolateral and posteromedial bundles. Isolated specimens were wrapped in saline-soaked gauze and frozen at –20°C until the day of mechanical testing. Ligaments from the contralateral knee of a single donor (female, aged 9 years) were used for microstructural analysis. Hematoxylin and eosin (H&E) histology, polarized light microscopy, and transmission electron microscopy (TEM) analyses were performed on the MCL, LCL, and PCL that were contralateral to the ligament samples used for mechanical testing.

Mechanical Testing

In preparation for mechanical testing, specimens were defrosted and cut into standardized dog-bone shapes at the midsubstance with a custom-built jig (Figure 1A). Cross-sectional areas were measured with a noncontact laser-based measurement system (Figure 1A). Specimen ends were gripped in custom aluminum clamps with 3-dimensionally printed plastic serrated jaws. The clamps

§Address correspondence to Michael W. Hast, PhD, Biedermann Laboratory for Orthopaedic Research, Department of Orthopaedic Surgery, University of Pennsylvania, 3737 Market Street, Suite 1050, Philadelphia, PA 19104, USA (email: hast@pennmedicine.upenn.edu).
*Biedermann Laboratory for Orthopaedic Research, Department of Orthopaedic Surgery, University of Pennsylvania, Philadelphia, Pennsylvania, USA.
†Children's Hospital of Philadelphia, Philadelphia, Pennsylvania, USA.
‡Department of Orthopaedic Surgery, Stanford University, Stanford, California, USA.
One or more of the authors has declared the following potential conflict of interest or source of funding: This study was supported by the Penn Center for Musculoskeletal Disorders Histology Core (NIH P30-AR06919) and the Electron Microscopy Resource Laboratory of the University of Pennsylvania, and were pediatric tissues were donated by AlloSource. T.J.G. receives research support from AlloSource, Vericel, and Liberty Surgical and has received hospitality payments from Arthrex. K.G.S. has received research support from AlloSource, Vericel, DePuy Synthes, and Sanofi-Aventis and is an unpaid consultant for Clinical Data Solutions and Source Trust. M.W.H. receives research support from DePuy Synthes, Integra LifeSciences, and Zimmer Biomet. AOSSM checks author disclosures against the Open Payments Database (OPD). AOSSM has not conducted an independent investigation on the OPD and disclaims any liability or responsibility relating thereto.
Ethical approval was not sought for the present study.

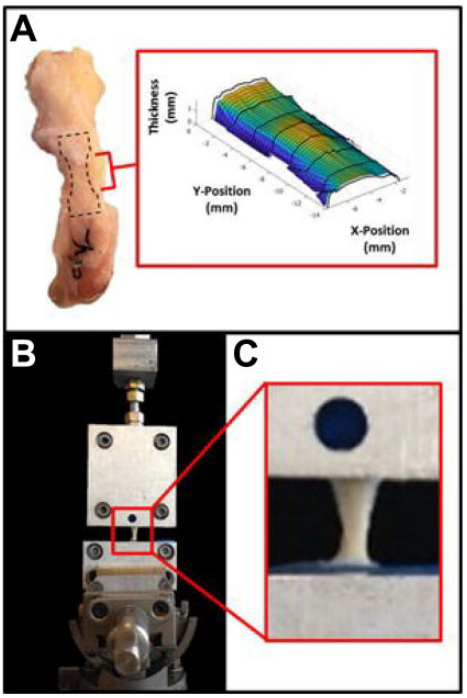

Figure 1. (A) Representative image of a harvested pediatric medial collateral ligament specimen. The dashed lines indicate the location where the specimen was cut into dog-bone shapes at the midsubstance. The cross-sectional area of the gauge length was measured using the topography generated from a laser-based 3-dimensional scanner. (B, C) Photograph of the tensile testing setup showing how the specimen was clamped and attached to the universal testing frame.

were then secured to a universal testing frame (ElectroForce 3330; TA Instruments) equipped with a 3-kN load cell (Figure 1, B and C). Tissues were kept hydrated throughout sample preparation and mechanical testing.

The tensile loading protocol was performed in accordance with a previously established method.[31] First, a 5-N preload was applied to the tissue from a slack starting position. The specimen underwent 10 preconditioning cycles between 5 and 10 N at a 0.4% strain rate. After relaxing at 5 N for 300 seconds, the specimen underwent a stress-relaxation protocol in which a 5% strain was applied for 1 second, followed by a hold for 300 seconds. The specimen was then allowed to rest at a 0% strain for 60 seconds before a ramp to failure was performed at 0.03% strain per second (Appendix Figure A1). Failure of the specimen was confirmed by an instantaneous decrease in force exceeding 50% of the total value. The known gauge length of the dog-bone ligament and the change in displacement of the actuator on the universal testing machine were used to determine the global longitudinal strain. The percentage of relaxation during the stress relaxation protocol was calculated as the percentage of change in stress from peak stress to equilibrium. The following bilinear constitutive model with a least squares fit, as utilized by similar studies,[9,25,43] was applied to the stress-strain data:

$$\sigma = \begin{cases} E\varepsilon & \varepsilon \le \varepsilon^* \\ E'(\varepsilon - \varepsilon^*) + E\varepsilon^* & \varepsilon > \varepsilon^* \end{cases},$$

where E is the slope of the toe modulus, E' is the slope of the Young modulus, ε is the strain, ε^* is the transition strain, and σ is the stress. This allowed for the quantification of the moduli in the toe and linear regions as well as a reasonable approximation of the stress and strain values corresponding to the transition point[9] (Appendix Figure A1). Stiffness was calculated as the slope of the load-displacement linear region. Strain energy density, which represents the energy absorbed before failure, was also considered and calculated as the area under the stress-strain curve.

Histology and Polarized Light Microscopy

Histology samples were fixed in 10% neutral buffered formalin, embedded in paraffin, serially sectioned ($\sim$8 μm), and stained with H&E for viewing under bright-field microscopy (Appendix Figure A2). Cell density in 10 randomly chosen regions (0.35 × 0.26 mm^2 each) was evaluated for each specimen using ImageJ software (National Institutes of Health). To analyze collagen crimp morphology, specimens were examined with polarized light microscopy using techniques previously described in the literature.[26] Images from 10 randomly chosen regions (0.35 × 0.26 mm^2 each) were obtained, and crimp wavelengths, which were calculated as the distance spanned by discrete dark and light band units (Appendix Figure A2),[12,49] were consecutively measured and averaged. For each specimen, a minimum of 100 individual crimps was analyzed.

Transmission Electron Microscopy

Samples for the electron microscopic examination were fixed overnight at 4°C with 2.5% glutaraldehyde and 2.0% paraformaldehyde in 0.1 M sodium cacodylate buffer. After subsequent buffer washes, the samples were post-fixed in 2.0% osmium tetroxide and rinsed in DH_2O before en bloc staining with 2% uranyl acetate. The tissues were then dehydrated through a graded ethanol series and embedded in EMbed 812 (Electron Microscopy Sciences). Thin sections were cut perpendicular to the longitudinal axis of the sample and stained with uranyl acetate and lead citrate. An electron microscope (JEOL 1010; JEOL USA) fitted with a digital camera and custom software (AMT Advantage; Advanced Microscopy Techniques) was used to capture images.

Ten images of the collagen fibril cross sections were obtained at 60,000× for each specimen, and each image was analyzed using a semiautomated protocol developed in ImageJ/Fiji software (Appendix Figure A2).[37] Specifically, a machine learning classifier was trained to separate the stained fibrils from the lighter background of the image. Using binary thresholding and watershed segmentation algorithms, the fibrils were completely segmented into discrete units. Individual fibers were fit with an ellipse, and the Feret minor diameter was calculated in an effort to

TABLE 1
Results for Pediatric MCLs, LCLs, and PCLs Obtained From Uniaxial Tensile Testing[a]

		Viscoelastic Property	Toe Region			Linear Region and Ultimate Mechanical Properties				
	n	Stress Relaxation, %	Transition Stress, MPa	Transition Strain, MPa	Toe Modulus, MPa	Ultimate Stress, MPa	Ultimate Strain, %	Young Modulus, MPa	Stiffness, N/mm	Strain Energy Density, MPa
MCL	5	29.8 ± 7.7	1.5 ± 0.5	3.5 ± 0.5	40.4 ± 20.0	11.7 ± 6.7	18.2 ± 6.8	93.7 ± 56.5	28.6 ± 6.1	1.2 ± 0.9
LCL	5	30.3 ± 7.0	1.2 ± 0.9	3.1 ± 1.0	31.8 ± 34.6	11.4 ± 11.5	27.7 ± 12.9	64.4 ± 76.6	30.8 ± 37.5	1.3 ± 1.0
PCL	5	28.7 ± 5.1	0.5 ± 0.2	2.8 ± 0.5	12.8 ± 5.2	4.2 ± 1.8	28.8 ± 11.9	19.8 ± 10.4	19.8 ± 10.8	0.7 ± 0.4
P values										
MCL vs LCL		.92	.87	.67	.57	.96	.38	.36	.88	.87
MCL vs PCL		.96	.02[b]	.36	.24	.39	.38	.02[b]	.80	.53
LCL vs PCL		.98	.27	.46	.39	.30	.88	.77	.84	.56

[a]Data are reported as mean ± SD unless otherwise specified. LCL, lateral collateral ligament; MCL, medial collateral ligament; PCL, posterior collateral ligament.
[b]Statistically significant difference ($P < .05$).

reduce errors introduced by unintentional oblique sectioning of the fibrils. Fibril diameter distributions were fit using kernel density estimation to highlight the modality of their profiles. Between 3000 and 7000 fibrils were analyzed over the 10 TEM images for each specimen.

Statistical Analysis

Because of the small sample size in this study, the statistical power was low. However, the rarity of pediatric cadaveric tissue precluded our ability to obtain a larger sample size. One-way analyses of variance ($\alpha = 0.05$) were performed to determine if there were any statistical differences between the mechanical property results for the MCL, LCL, and PCL. For data that passed the Shapiro-Wilk test for normality ($\alpha = 0.05$) and the Brown-Forsythe test for equal variance ($\alpha = 0.05$), a post hoc Holm-Sidak test was used to perform multiple comparisons. If the criteria for normality and equal variance were not met, the Kruskal-Wallis test was used instead of 1-way analysis of variance, and a post hoc Dunn test was used to perform multiple comparisons.

RESULTS

Mechanical Testing

Failure for all specimens occurred in the midsubstance of the dog-bone ligament. The pediatric PCL exhibited mechanical properties that were weaker than the MCL and LCL, particularly for ultimate stress, the Young modulus, and strain energy density (Table 1 and Appendix Table A1). Transition stress, transition strain, and the toe modulus for the PCL also had the weakest values between the 3 ligaments (Table 1 and Appendix Table A2). Although variations between measurements were fairly low for the MCL and PCL, large variations were observed for ultimate stress, the Young modulus, and stiffness for the LCL. Stress relaxation values were similar for all 3 ligaments.

Histology, Polarized Light Microscopy, and TEM

Each of the tissues tested exhibited unique microstructural characteristics. Cell density analysis of H&E-stained sections showed higher mean concentrations of fibroblasts in the LCL compared with the MCL and PCL (Figure 2). Polarized light microscopy indicated that crimp wavelengths were uniform, with low amounts of intrafiber variation within the same specimen. Additionally, mean crimp wavelengths were very similar between the different ligaments. Mean collagen fibril diameters were also comparable between ligament types; however, the modality of these fibril diameter sizes was noticeably distinct. Specifically, the MCL displayed a tightly bundled unimodal profile, while the PCL displayed a wider and more even range of fibril diameters, and the LCL exhibited a distinctly bimodal profile.

DISCUSSION

Comparing the mechanical characteristics from this study to similar measures obtained in adult cohorts provides much-needed elucidation on the differences between adult and pediatric ligaments. Results from this study demonstrated that the mechanical properties of the pediatric MCL, LCL, and PCL were considerably weaker than what has been documented in healthy adult populations from studies that were similar in methodology (Figure 3 and Table 2). Specifically, 2 previous studies[34,39] demonstrated average ultimate stress, ultimate strain, the Young modulus, and strain energy density from adult human MCL samples that were higher than our reported values for pediatric MCLs. They found that adult MCLs had a significantly higher Young modulus than LCLs, which agrees with the results from this study. Interestingly, the adult MCLs had lower strain energy density than the LCLs, but our findings suggest that these values are similar in the pediatric samples we tested. The reported average ultimate strain values from the adult studies were very similar to what was documented in this study of pediatric samples. The variability in mechanical properties for the pediatric LCL described in

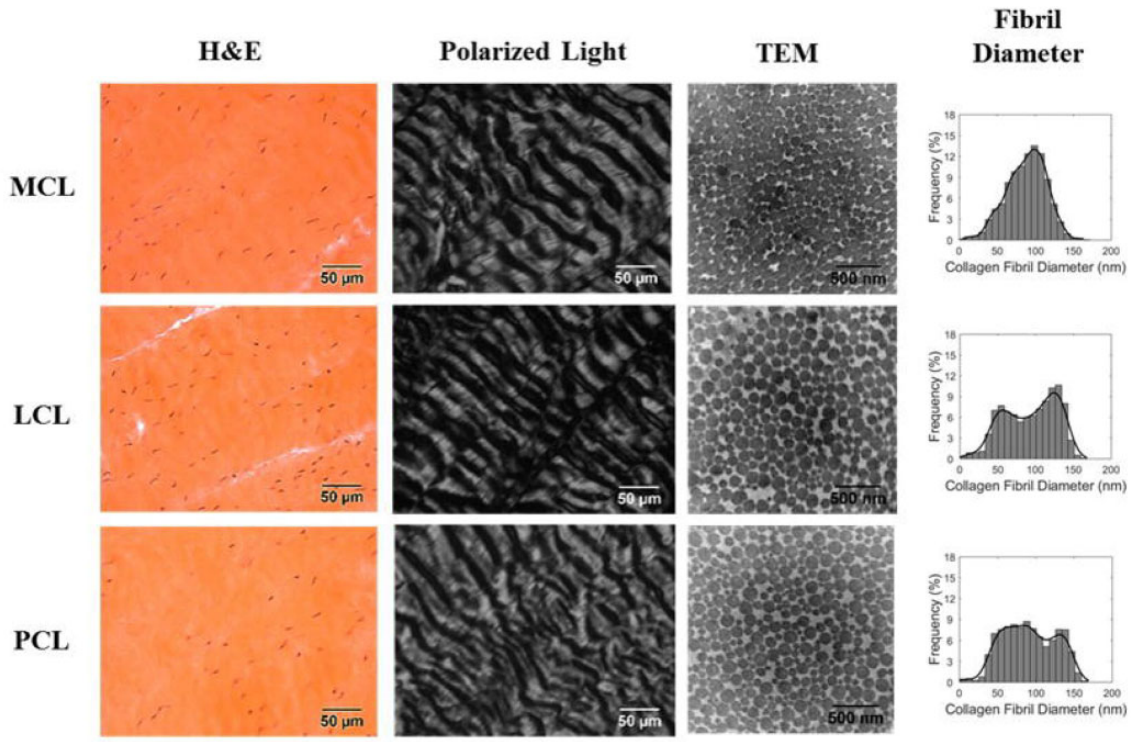

	Fibroblast Density (cells/mm^2)	Crimp Wavelength (μm)	Collagen Fibril Diameter (nm)
MCL	684.6 ± 90.7	32.8 ± 3.6	88.0 ± 26.0
LCL	1062.9 ± 85.6	27.2 ± 3.5	93.3 ± 34.6
PCL	804.5 ± 103.5	25.8 ± 3.5	90.9 ± 34.0

Figure 2. Microstructural results for the pediatric medial collateral ligament (MCL), lateral collateral ligament (LCL), and posterior collateral ligament (PCL) samples originating from 1 donor. First column: representative hematoxylin and eosin (H&E)–stained histology sections for each ligament. Second column: representative polarized light microscopy images of crimp morphology. Third column: representative transmission electron microscopy (TEM) images of collagen fibril cross sections. Fourth column: histograms showing the relative frequency of collagen fibril diameters. Bottom table: quantitative results from the microstructural analyses for each ligament.

this study made it difficult to compare with the other ligaments. Race and Amis[35] reported values for adult PCL anterolateral bundle stiffness, the Young modulus, and ultimate stress that were considerably larger than our data for the pediatric PCL.[35] To our knowledge, there are currently no data in the literature regarding the toe region properties for the adult or pediatric human MCL, LCL, or PCL. While the viscoelastic behavior of these structures may not be as clinically relevant as the mechanical properties that we report, it is interesting to note that there were remarkably similar viscoelastic responses between all 3 ligaments. Values for stress relaxation were similar to reported values for adult cohorts.[5,48]

It is more difficult to make direct comparisons of pediatric crimp morphology results to adult human and animal models because these data are extremely rare. The crimp wavelengths measured in this study were generally smaller than what has been documented for extra-articular tendons of the adult human knee, such as the patellar, quadriceps, and semitendinosus tendons.[1,18,40] They were also smaller than the crimp wavelengths observed for the pediatric versions of these tendons, which originated from the same donor and were featured in one of our previous studies.[38] However, they were comparable with the crimp wavelengths exhibited by the donor's ACL and iliotibial band (ITB) samples.[38]

There is a slightly deeper pool of data regarding the collagen fibril ultrastructure; however, most of these studies were conducted using animal models instead of human tissues. In these animal models, the fibril diameter size distribution shifts from a tightly clustered unimodal profile to a bimodal profile over the course of maturation.[14,43] It has been posited that this change is reflective of an adaptation to increased loading demands.[33] Collagen diameters for the pediatric MCL sample from the 9-year-old female specimen

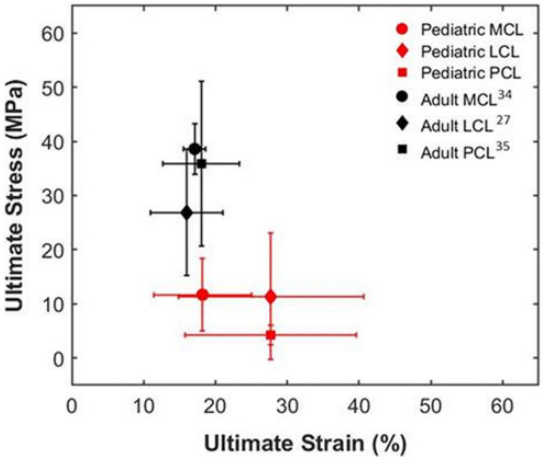

Figure 3. Ultimate stress-strain plot for the data presented in the current study (red points) compared with data reported in the adult population (black points). Data points represent the mean ultimate stress and ultimate strain. The vertical error bars indicate the standard deviation for ultimate stress, while the horizontal error bars indicate the standard deviation for ultimate strain.

in this study exhibited a distinctly unimodal profile. If the patterns observed in animal studies hold true in humans, it is possible that the MCL from this donor experienced low loads or had a more prolonged or delayed timeline for collagen maturation. The other ligament samples from this donor may have been exposed to higher loads or have different timelines of maturation. Specifically, the LCL appears to be approaching a bimodal distribution, while the PCL has already achieved this bimodal hallmark.

Microstructural characteristics of pediatric knee ligaments are not well described in the literature, but they are important to document because bioengineered constructs are most effective when they can fully mimic the tissue microstructure and mechanics.[42] The tight distribution of fibril diameters exhibited by the MCL from the 9-year-old donor most closely matches that of its ACL and ITB, as reported in our previous study.[38] From a biomimicry perspective, this microstructural evidence suggests that the ITB may be the most suitable graft particularly for MCL reconstruction/augmentation. Microstructural properties were evaluated in the tissues from only 1 donor, and definitive correlations between mechanical and microstructural results cannot be drawn without studies featuring larger sample sizes. More research is needed to complete this comprehensive data set of baseline data for both adult and adolescent ligament applications.

Although surgical intervention for collateral ligament tears in pediatric patients is rare, it has been reported that they can be addressed with primary suture repair and graft augmentation. Specifically, Gorin et al[17] presented a case report for a skeletally immature patient with a combined ACL-MCL injury that was surgically treated with gracilis autograft augmentation. Reported surgical techniques for pediatric PCL tears also include primary suture repair and reconstruction with Achilles tendon allografts.[22] Results from our previous study demonstrated that pediatric semitendinosus tendons and ITBs possess the strongest mechanical properties among other candidate grafts, including the quadriceps and patellar tendons.[38] In the context of graft augmentation in these pediatric ligaments, results indicate that the ITB may be an underutilized candidate. Not only does it possess similar microstructural properties to the native MCL, LCL, and PCL, but it would also provide the strength necessary to prevent reruptures of these ligaments. To our knowledge, there are no documented cases or reported clinical outcomes of using an ITB graft for collateral ligament or PCL reconstruction.

This study has several limitations that are worth acknowledging. First, the sample size in this experiment was low because of the rarity of these pediatric tissues. This constraint was exacerbated because specimens from the donor cohort were utilized by several different research institutions for various investigations. This challenge was unavoidable and prevented meaningful statistical comparisons of the different ligament structures. Second, direct comparisons between mechanical data from the current study and studies featuring adult cohorts are complicated by the lack of a standardized tendon/ligament tensile testing protocol. The differences in methodological variables can ultimately alter mechanical outcomes.[9,44] Ligament construct configuration is one of the main areas where protocols diverge. While some groups use potted bone-ligament-bone units that are intended to simulate complex in vivo loading, we chose to characterize the mechanical behavior of the ligament at the midsubstance with uniaxial tensile testing. By characterizing the intrinsic mechanical properties of the

TABLE 2
Mechanical Properties of Adult MCLs, LCLs, and PCLs Previously Reported in the Literature[a]

Study	Ligament	n	Ligament Preparation	Ultimate Stress, MPa	Ultimate Strain, %	Young Modulus, MPa	Strain Energy Density, MPa
Quapp and Weiss[34]	MCL	10	Midsubstance	38.6 ± 4.8	17.1 ± 1.5	332.2 ± 58.3	N/A
Smeets et al[39]	MCL	12	Midsubstance	72.4 ± 20.7	22.9 ± 2.5	441.8 ± 117.2	7.5 ± 2.9
Smeets et al[39]	LCL	12	Midsubstance	83.6 ± 38.1	41.0 ± 9.9	289.0 ± 159.7	15.2 ± 6.4
LaPrade et al[27]	LCL	8	Bone-ligament-bone	26.9 ± 11.7	15.0 ± 5.0	183.5 ± 110.7	N/A
Race and Amis[35b]	PCL	7	Bone-ligament-bone	35.9 ± 15.2	18.0 ± 5.3	248.0 ± 119.0	N/A

[a]Data are reported as mean ± SD unless otherwise specified. LCL, lateral collateral ligament; MCL, medial collateral ligament; N/A, not available; PCL, posterior collateral ligament.
[b]Results reported for the anterior bundle of the PCL.

tissue, we were able to eliminate confounding variables related to individual variation in tissue geometry and insertion properties and present values that are more representative of underlying collagen behavior and morphology. From a clinical perspective, however, high-grade injuries to these pediatric tissues are more likely to involve an avulsion than a midsubstance failure,[10,45] and an investigation into the failure properties of femoral and tibial insertions would be a good direction for future research. Additional studies should also investigate the ultimate force of these pediatric ligaments based on their native cross-sectional areas, as this can also be an informative metric for clinicians. The specimens in this study were cut into dog-bone shapes before testing (to ensure that failure occurred in the midsubstance of the tissue). Consequently, values for ultimate stress were more appropriate to report here.

Mechanical properties are also known to be dependent on the stain rate,[4,21] and previous knee tendon and ligament studies have utilized ramp-to-failure strain rates of 100% per second or higher to replicate the fast strain rates that are thought to occur during acute injuries.[4,19,32] To minimize viscoelastic effects and capture better approximations of toe region properties, we instead adopted a quasistatic strain rate of 0.03% per second. In this study, strain was calculated using grip-to-grip displacement; however, measurements of local strain can also be taken into consideration and calculated using fiducial markers and optical tracking techniques. Future research should involve evaluating the behavior of the collagen microstructure simultaneous to tensile testing in conjunction with these optical techniques, which would offer a more complete picture of ligament dynamics for these pediatric specimens. Last, the ligaments examined in this study were acquired from donors aged 7 to 11 years, and it may not be appropriate to apply the results from this study to younger or older age groups without additional research. Donor activity level and cause of death may also have an effect on the mechanical and microstructural results of this study. This information could have improved the interpretation of data; however, it was unavailable.

CONCLUSION

This study represents the second iteration of an experimental protocol that utilized a small and extremely rare sample of pediatric cadaveric knees. The findings from this study help to address the knowledge gap with respect to the biomechanical and microstructural properties of pediatric MCLs, LCLs, and PCLs. Our data showed that the pediatric MCL and LCL possessed similar mechanical properties, while the pediatric PCL was slightly weaker. All 3 of these pediatric structures were weaker than what has been reported in studies featuring adult cohorts. The optimization of treatment for injuries to these ligaments continues to evolve and will benefit significantly from a comprehensive data set of these properties. These findings may provide practicing surgeons with more informed choices when selecting grafts for reconstruction. Additionally, researchers in the areas of computational simulations and the design and fabrication of biomimetic synthetic constructs will benefit from this information.

REFERENCES

1. Abe S, Kurosaka M, Iguchi T, Yoshiya S, Hirohata K. Light and electron microscopic study of remodeling and maturation process in autogenous graft for anterior cruciate ligament reconstruction. *Arthroscopy*. 1993;9(4):394-405.
2. Allen CR, Kaplan LD, Fluhme DJ, Harner CD. Posterior cruciate ligament injuries. *Curr Opin Rheumatol*. 2002;14(2):142-149.
3. Anderson AF, Anderson CN. Posterior cruciate and posterolateral ligament reconstruction in an adolescent with open physes: a case report. *J Bone Joint Surg Am*. 2007;89(7):1598-1604.
4. Blevins FT, Hecker AT, Bigler GT, Boland AL, Hayes WC. The effects of donor age and strain rate on the biomechanical properties of bone-patellar tendon-bone allografts. *Am J Sports Med*. 1994;22(3):328-333.
5. Bonifasi-Lista C, Lakez SP, Small MS, Weiss JA. Viscoelastic properties of the human medial collateral ligament under longitudinal, transverse and shear loading. *J Orthop Res*. 2005;23(1):67-76.
6. Bosch U, Decker B, Kasperczyk W, Nerlich A, Oestern H-J, Tscherne H. The relationship of mechanical properties to morphology in patellar tendon autografts after posterior cruciate ligament replacement in sheep. *J Biomech*. 1992;25(8):821-830.
7. Bovid KM, Salata MJ, Vander Have KL, Sekiya JK. Arthroscopic posterior cruciate ligament reconstruction in a skeletally immature patient: a new technique with case report. *Arthroscopy*. 2010;26(4):563-570.
8. Caine D, Maffulli N, Caine C. Epidemiology of injury in child and adolescent sports: injury rates, risk factors, and prevention. *Clin Sports Med*. 2008;27(1):19-50.
9. Chandrashekar N, Hashemi J, Slauterbeck J, Beynnon BD. Low-load behaviour of the patellar tendon graft and its relevance to the biomechanics of the reconstructed knee. *Clin Biomech*. 2008;23(7):918-925.
10. Cosgarea AJ, Jay PR. Posterior cruciate ligament injuries: evaluation and management. *J Am Acad Orthop Surg*. 2001;9(5):297-307.
11. Covey CD, Sapega AA. Injuries of the posterior cruciate ligament. *J Bone Joint Surg Am*. 1993;75(9):1376.
12. Diamant J, Keller A, Baer E, Litt M, Arridge RGC. Collagen: ultrastructure and its relation to mechanical properties as a function of ageing. *Proc R Soc Lond B Biol Sci*. 1972;180(1060):293-315.
13. Eleswarapu SV, Responte DJ, Athanasiou KA. Tensile properties, collagen content, and crosslinks in connective tissues of the immature knee joint. *PLoS One*. 2011;6(10):e26178.
14. Frank C, Bray D, Rademaker A, et al. Electron microscopic quantification of collagen fibril diameters in the rabbit medial collateral ligament: a baseline for comparison. *Connect Tissue Res*. 1989;19(1):11-25.
15. Frank C, Strother R. Isolated posterior cruciate ligament injury in a child: literature review and a case report. *Can J Surg*. 1989;32(5):373-374.
16. Goodrich AMD, Ballard AMD. Posterior cruciate ligament avulsion associated with ipsilateral femur fracture in a 10-year-old child. *J Trauma*. 1988;28(9):1393-1396.
17. Gorin S, Paul DD, Wilkinson EJ. An anterior cruciate ligament and medial collateral ligament tear in a skeletally immature patient: a new technique to augment primary repair of the medial collateral ligament and an allograft reconstruction of the anterior cruciate ligament. *Arthroscopy*. 2003;19(10):E21-E26.
18. Hadjicostas PT, Soucacos PN, Koleganova N, Krohmer G, Berger I. Comparative and morphological analysis of commonly used autografts for anterior cruciate ligament reconstruction with the native ACL: an electron, microscopic and morphologic study. *Knee Surg Sports Traumatol Arthrosc*. 2008;16(12):1099-1107.
19. Hashemi J, Chandrashekar N, Mansouri H, Slauterbeck JR, Hardy DM. The human anterior cruciate ligament: sex differences in ultrastructure and correlation with biomechanical properties. *J Orthop Res*. 2008;26(7):945-950.

20. Ingram JG, Fields SK, Yard EE, Comstock RD. Epidemiology of knee injuries among boys and girls in US high school athletics. *Am J Sports Med*. 2008;36(6):1116-1122.
21. Kahn CJF, Wang X, Rahouadj R. Nonlinear model for viscoelastic behavior of Achilles tendon. *J Biomech Eng*. 2010;132(11):111002.
22. Kocher MSM, Shore B, Nasreddine AY, Heyworth BE. Treatment of posterior cruciate ligament injuries in pediatric and adolescent patients. *J Pediatr Orthop*. 2012;32(6):553-560.
23. Kramer DE, Miller PE, Berrahou IK, Yen Y-M, Heyworth BE. Collateral ligament knee injuries in pediatric and adolescent athletes [published online December 8, 2017]. *J Pediatr Orthop*. doi:10.1097/BPO.0000000000001112
24. Kraus T, Švehlík M, Singer G, Schalamon J, Zwick E, Linhart W. The epidemiology of knee injuries in children and adolescents. *Arch Orthop Trauma Surg*. 2012;132(6):773-779.
25. Lake SP, Miller KS, Elliott DM, Soslowsky LJ. Effect of fiber distribution and realignment on the nonlinear and inhomogeneous mechanical properties of human supraspinatus tendon under longitudinal tensile loading. *J Orthop Res*. 2009;27(12):1596-1602.
26. Lake SP, Miller KS, Elliott DM, Soslowsky LJ. Tensile properties and fiber alignment of human supraspinatus tendon in the transverse direction demonstrate inhomogeneity, nonlinearity and regional isotropy. *J Biomech*. 2010;43(4):727-732.
27. LaPrade RF, Muench C, Wentorf F, Lewis JL. The effect of injury to the posterolateral structures of the knee on force in a posterior cruciate ligament graft: a biomechanical study. *Am J Sports Med*. 2002;30(2):233-238.
28. LaPrade RF, Resig S, Wentorf F, Lewis JL. The effects of grade III posterolateral knee complex injuries on anterior cruciate ligament graft force. *Am J Sports Med*. 1999;27(4):469-475.
29. LaPrade RF, Spiridonov SI, Coobs BR, Ruckert PR, Griffith CJ. Fibular collateral ligament anatomical reconstructions: a prospective outcomes study. *Am J Sports Med*. 2010;38(10):2005-2011.
30. Meislin RJ. Managing collateral ligament tears of the knee. *Phys Sportsmed*. 1996;24(3):67-80.
31. Miller KS, Connizzo BK, Feeney E, Tucker JJ, Soslowsky LJ. Examining differences in local collagen fiber crimp frequency throughout mechanical testing in a developmental mouse supraspinatus tendon model. *J Biomech Eng*. 2012;134(4):41004.
32. Noyes FR, Grood ES. The strength of the anterior cruciate ligament in humans and Rhesus monkeys. *J Bone Joint Surg Am*. 1976;58(8):1074-1082.
33. Parry DAD. The molecular fibrillar structure of collagen and its relationship to the mechanical properties of connective tissue. *Biophys Chem*. 1988;29(1):195-209.
34. Quapp KM, Weiss JA. Material characterization of human medial collateral ligament. *J Biomech Eng*. 1998;120(6):757-763.
35. Race A, Amis AA. The mechanical properties of the two bundles of the human posterior cruciate ligament. *J Biomech*. 1994;27(1):13-24.
36. Robinson JR, Bull AM, Amis AA. Structural properties of the medial collateral ligament complex of the human knee. *J Biomech*. 2005;38(5):1067-1074.
37. Schindelin J, Arganda-Carreras I, Frise E, et al. Fiji: an open source platform for biological image analysis. *Nat Methods*. 2012;9(7):676-682.
38. Schmidt EC, Chin M, Aoyama JT, Ganley TJ, Shea KG, Hast MW. Mechanical and microstructural properties of pediatric anterior cruciate ligaments and autograft tendons used for reconstruction. *Orthop J Sports Med*. In press.
39. Smeets K, Slane J, Scheys L, Claes S, Bellemans J. Mechanical analysis of extra-articular knee ligaments, part one: native knee ligaments. *Knee*. 2017;24(5):949-956.
40. Strocchi R, de Pasquale V, Gubellini P, et al. The human anterior cruciate ligament: histological and ultrastructural observations. *J Anat*. 1992;180(pt 3):515-519.
41. Swenson DM, Collins CL, Best TM, Flanigan DC, Fields SK, Comstock RD. Epidemiology of knee injuries among U.S. high school athletes, 2005/2006-2010/2011. *Med Sci Sports Exerc*. 2013;45(3):462-469.
42. Szczesny SE, Driscoll TP, Tseng H-Y, et al. Crimped nanofibrous biomaterials mimic microstructure and mechanics of native tissue and alter strain transfer to cells. *ACS Biomater Sci Eng*. 2017;3(11):2869-2876.
43. Wan C, Hao Z, Wen S, Leng H. A quantitative study of the relationship between the distribution of different types of collagen and the mechanical behavior of rabbit medial collateral ligaments. *PLoS One*. 2014;9(7):e103363.
44. West RV, Harner CD. Graft selection in anterior cruciate ligament reconstruction. *J Am Acad Orthop Surg*. 2005;13(3):197-207.
45. Wilson TC, Satterfield WH, Johnson DL. Medial collateral ligament "tibial" injuries: indication for acute repair. *Orthopedics*. 2004;27(4):389-393.
46. Wilson WT, Deakin AH, Payne AP, Picard F, Wearing SC. Comparative analysis of the structural properties of the collateral ligaments of the human knee. *J Orthop Sports Phys Ther*. 2012;42(4):345-351.
47. Woo SL-Y, Ohland KJ, Weiss JA. Aging and sex-related changes in the biomechanical properties of the rabbit medial collateral ligament. *Mech Ageing Dev*. 1990;56(2):129-142.
48. Wright JO, Skelley NW, Schur RP, Castile RM, Lake SP, Brophy RH. Microstructural and mechanical properties of the posterior cruciate ligament: a comparison of the anterolateral and posteromedial bundles. *J Bone Joint Surg Am*. 2016;98(19):1656.
49. Zhao L, Thambyah A, Broom N. Crimp morphology in the ovine anterior cruciate ligament. *J Anat*. 2015;226(3):278-288.

APPENDIX

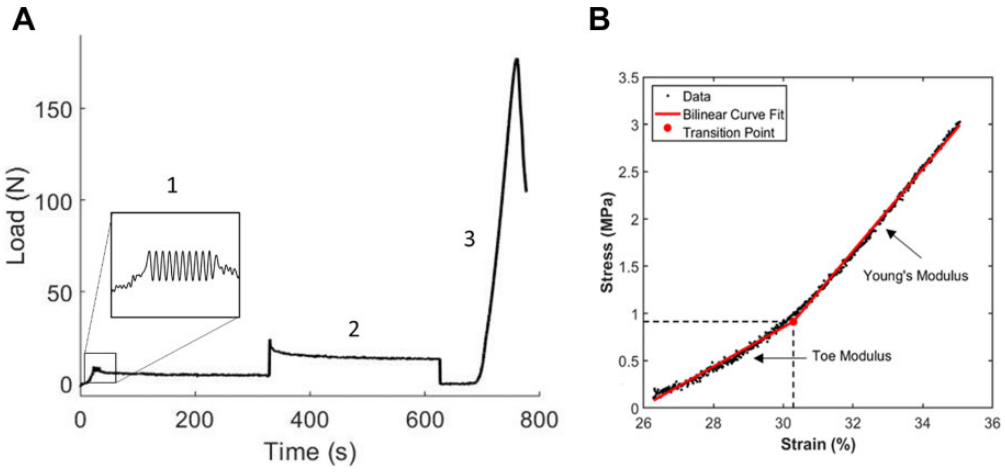

Figure A1. Schematic of the mechanical testing protocol. (A) Specimens were subjected to (1) preconditioning, (2) stress relaxation, and (3) ramp-to-failure phases. (B) The stress-strain data from the ramp to failure can be fit using a bilinear constitutive model to approximate the moduli in the toe and linear regions as well as the transition point.

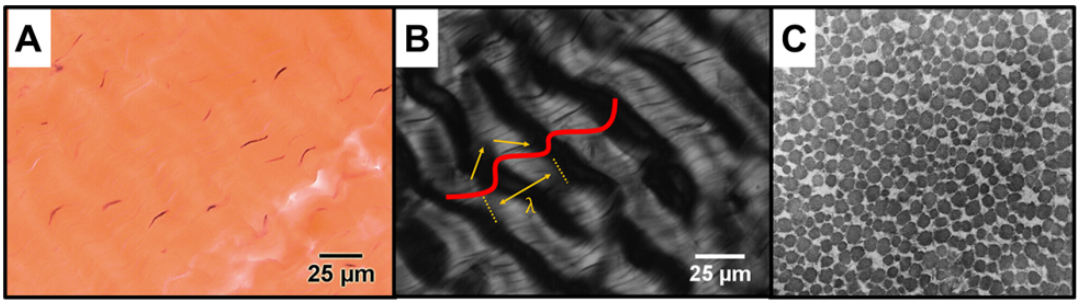

Figure A2. (A) Representative bright-field microscopy image of a hematoxylin and eosin–stained pediatric medial collateral ligament (MCL). Fibroblast nuclei are stained purple. (B) Representative polarized light microscopy image of a pediatric MCL showing how the discrete crimps are identified. The crimp wavelength (λ) is measured in micrometers. (C) Representative transmission electron microscopy image of a pediatric MCL sample.

TABLE A1
Results for Pediatric MCLs, LCLs, and PCLs Obtained From Tensile Testing[a]

Donor	Age, y	Sex	CSA, mm^2	Stress Relaxation, %	Ultimate Stress, MPa	Ultimate Strain, %	Young Modulus, MPa	Stiffness, N/mm	Strain Energy Density, MPa
MCL									
1	7	F	4.8	42.0	18.9	18.1	114.6	27.0	1.4
2	11	M	9.3	22.6	3.9	8.8	61.3	21.7	0.2
3	10	M	11.8	30.6	5.9	16.2	48.9	29.6	0.5
4	9	M	9.5	24.0	12.2	27.4	59.9	26.3	1.8
5	9	F	5.7	30.0	17.5	20.5	183.8	38.2	2.3
LCL									
1	7	F	8.4	27.1	5.3	21.9	32.2	16.0	0.6
2	11	M	10.0	28.2	6.0	21.3	35.3	19.5	0.7
3	10	M	9.7	37.1	9.9	26.0	47.1	18.0	1.2
4	9	M	9.2	37.6	4.2	50.3	8.1	3.7	1.1
5	9	F	8.8	21.3	31.5	19.2	199.1	96.9	3.0
PCL									
1	7	F	12.2	25.3	6.0	21.9	37.1	38.2	0.7
2	11	M	19.6	35.2	4.3	47.6	11.7	13.8	1.0
3	10	M	14.5	24.5	2.4	21.8	15.2	12.2	0.3
4	9	M	12.9	33.1	2.4	19.2	13.0	14.2	0.3
5	9	F	12.4	25.3	5.8	33.7	22.0	20.9	1.2

[a]CSA, cross-sectional area; F, female; LCL, lateral collateral ligament; M, male; MCL, medial collateral ligament; PCL, posterior collateral ligament.

TABLE A2
Toe Region Results for Pediatric MCLs, LCLs, and PCLs Obtained From Tensile Testing[a]

Donor	Age, y	Sex	Transition Stress, MPa	Transition Strain, %	Toe Modulus, MPa
MCL					
1	7	F	1.5	3.9	41.0
2	11	M	1.5	3.5	35.5
3	10	M	0.9	4.0	20.6
4	9	M	1.2	3.1	31.1
5	9	F	2.3	3.0	73.5
LCL					
1	7	F	1.0	3.4	20.5
2	11	M	1.0	3.7	19.3
3	10	M	0.8	4.1	18.1
4	9	M	0.3	1.5	8.0
5	9	F	2.8	3.0	93.1
PCL					
1	7	F	0.7	2.9	20.6
2	11	M	0.3	3.0	7.4
3	10	M	0.4	1.9	10.3
4	9	M	0.5	3.0	10.1
5	9	F	0.7	3.2	15.3

[a]F, female; LCL, lateral collateral ligament; M, male; MCL, medial collateral ligament; PCL, posterior collateral ligament.